Electronic Supplementary Information (ESI)

Investigation of transitions between the M-phases in $AgNbO_3$ based ceramics

Zhongna Yan, Dou Zhang, Xuefan Zhou, Man Zhang, Ludan Zhang, Hangfeng Zhang, Guoliang Xue, Isaac Abrahams and Haixue Yan

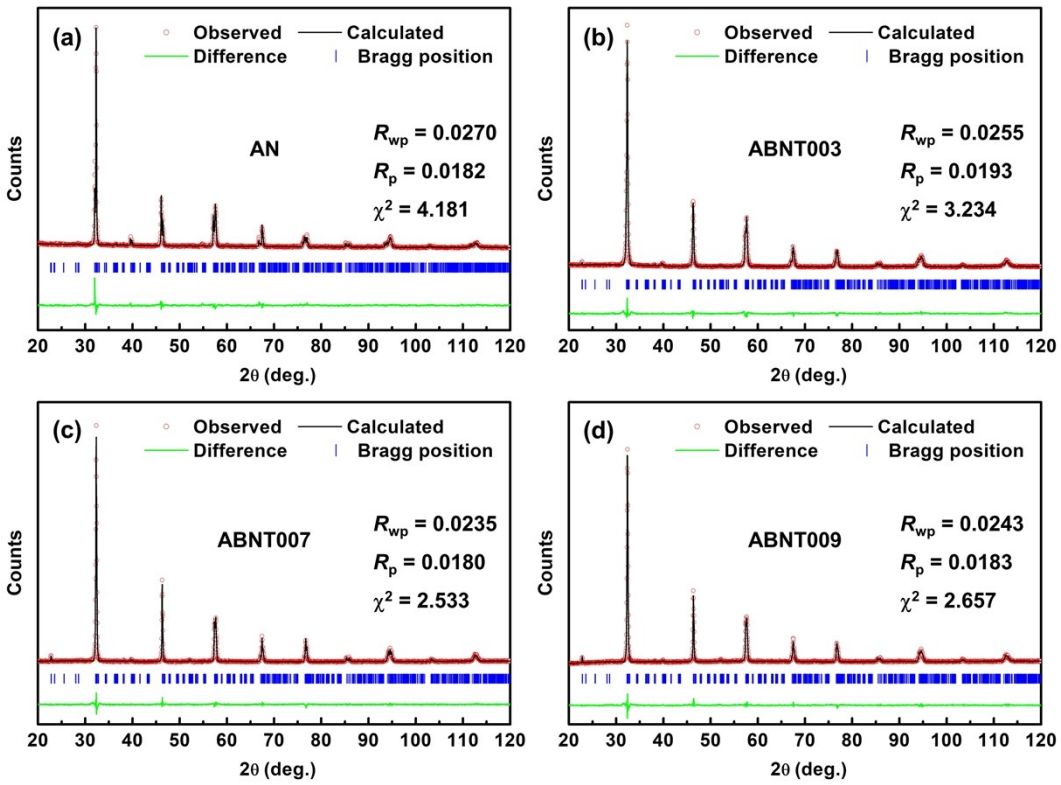

Fig. S1 Fitted room temperature diffraction profiles for AN and ABNT*x* ceramic powders using space groups $Pb2_1m$ for AN and *Pbcm* for ANBC*x*.

Table S1 Crystal and refinement parameters for AN and ABNT*x* ceramic powders at room temperature. Estimated standard deviations are given in parentheses.

Chemical formula	$AgNbO_3$	$Ag_{0.91}Bi_{0.03}Nb_{0.8}Ta_{0.2}O_3$	$Ag_{0.79}Bi_{0.07}Nb_{0.8}Ta_{0.2}O_3$	$Ag_{0.73}Bi_{0.09}Nb_{0.8}Ta_{0.2}O_3$
Formula weight	248.771 g mol^{-1}	262.941 g mol^{-1}	258.356 g mol^{-1}	256.063 g mol^{-1}
Crystal system	Orthorhombic	Orthorhombic	Orthorhombic	Orthorhombic
Space group	*Pb*2$_1$*m*	*Pbcm*	*Pbcm*	*Pbcm*
Unit cell dimensions	*a* = 5.548(2) Å *b* = 5.605(1) Å *c* = 15.662(4)Å	*a* = 5.540(2) Å *b* = 5.590(2) Å *c* = 15.709(6)Å	*a* = 5.538(1) Å *b* = 5.582(1) Å *c* = 15.730(3)Å	*a* = 5.540(1) Å *b* = 5.580(2) Å *c* = 15.736(5)Å
Volume	487.0(3) Å^3	486.4(3) Å^3	486.3(2) Å^3	486.5(3) Å^3
Z[a]	8	8	8	8
Density (calculated)	6.785 g cm^{-3}	7.181 g cm^{-3}	7.058 g cm^{-3}	6.993g cm^{-3}
R-factors[b]	R_{wp} = 0.0270 R_p = 0.0182 R_{ex} = 0.0133 R_{F^2} = 0.2297 χ^2 = 4.181	R_{wp} = 0.0255 R_p = 0.0193 R_{ex} = 0.0142 R_{F^2} = 0.1252 χ^2 = 3.234	R_{wp} = 0.0235 R_p = 0.0180 R_{ex} = 0.0148 R_{F^2} = 0.0715 χ^2 = 2.533	R_{wp} = 0.0243 R_p = 0.0183 R_{ex} = 0.0150 R_{F^2} = 0.0724 χ^2 = 2.657
Total number of variables	34	28	28	28
No. of profile points used	3331	3331	3331	3331
No. of reflections	856	761	758	760

[a]*Z* = the number of formula units per cell;

[b]For definition of *R*-factors see A.C. Larson and R.B. Von Dreele, Report No. LAUR 86-748. Program GSAS for Windows, Version 15-04-04. Los Alamos National Laboratory, New Mexico, USA, 1987.

Table S2 Selected bond lengths (Å) and angles (°) for AN and ABNT*x* ceramics in space groups $Pb2_1m$ and *Pbcm*, respectively. Data were collected on crushed samples at room temperature.

AN		ABNT003		ABNT007		ABNT009	
Ag1-O1	2.498(18)	Ag1-O1	2.620(16)	Ag1-O1	2.586(18)	Ag1-O1	2.577(22)
Ag1-O4	2.452(14)	Ag1-O1′	2.366(34)	Ag1-O1′	2.365(32)	Ag1-O1′	2.355(24)
Ag1-O6	2.358(13)	Ag1-O3	2.701(21) × 2	Ag1-O3	2.687(20) × 2	Ag1-O3	2.678(17) × 2
Ag1-O7	2.707(14)	Ag1-O4	2.633(19) × 2	Ag1-O4	2.652(19) × 2	Ag1-O4	2.662(18) × 2
Ag2-O2	2.64(10)	Ag1-O4′	2.554(21) × 2	Ag1-O4′	2.541(20) × 2	Ag1-O4′	2.545(17) × 2
Ag2-O2	2.412(30)	Ag2-O2	2.328(34)	Ag2-O2	2.323(32)	Ag2-O2	2.334(24)
Ag2-O3	2.41(6) × 2	Nb1-O1	2.017(14)	Nb1-O1	2.019(13)	Nb1-O1	2.028(13)
Ag3-O5	2.386(25)	Nb1-O2	2.012(14)	Nb1-O2	2.016(13)	Nb1-O2	2.010(13)
Ag3-O7	2.55(6)	Nb1-O3	1.598(19)	Nb1-O3	1.588(17)	Nb1-O3	1.593(12)
Nb1-O1	1.859(12)	Nb1-O3′	2.353(19)	Nb1-O3′	2.360(17)	Nb1-O3′	2.382(12)
Nb1-O5	2.131(13)	Nb1-O4	1.993(19)	Nb1-O4	1.983(17)	Nb1-O4	1.961(12)
Nb1-O6	1.96(5)	Nb1-O4′	1.973(18)	Nb1-O4′	1.979(17)	Nb1-O4′	1.976(12)
Nb1-O6′	2.07(5)	Nb1-Bi1	3.434(19)	Nb1-Bi1	3.446(17)	Nb1-Bi1	3.442(20)
Nb1-O7	1.96(5)	Nb1-Bi1	3.397(19)	Nb1-Bi1	3.380(16)	Nb1-Bi1	3.387(19)
Nb1-O7′	2.03(5)	Nb1-Bi1	3.403(34)	Nb1-Bi1	3.400(31)	Nb1-Bi1	3.408(27)
Nb2-O1	1.986(16)	Nb1-Bi1	3.388(34)	Nb1-Bi1	3.391(31)	Nb1-Bi1	3.388(27)
Nb2-O2	1.975(18)	Nb1-Bi1	3.459(10)	Nb1-Bi1	3.449(10)	Nb1-Bi1	3.436(11)
Nb2-O3	1.96(7)	Nb1-Bi1	3.373(11)	Nb1-Bi1	3.382(10)	Nb1-Bi1	3.390(11)
Nb2-O3	2.02(6)	Nb1-Bi1	3.401(34)	Nb1-Bi1	3.407(31)	Nb1-Bi1	3.413(27)
Nb2-O4	1.90(5)	Nb1-Bi1	3.390(34)	Nb1-Bi1	3.389(31)	Nb1-Bi1	3.381(27)
Nb2-O4′	2.12(7)	Nb1-O1-Nb1	153.6(13)	Nb1-O1-Nb1	153.3(12)	Nb1-O1-Nb1	152.1(7)
Nb1-O1-Nb2	161.6(9)	Nb1-O1-Ta1	0.000(0)	Nb1-O1-Ta1	0.000(0)	Nb1-O1-Ta1	0.000(0)
Nb2-O2-Nb2	154.8(25)	Nb1-O1-Ta1	153.6(13)	Nb1-O1-Ta1	153.3(12)	Nb1-O1-Ta1	152.1(7)
Nb2-O3-Nb2	160.6(26)	Nb1-O1-Bi1	93.31(30)	Nb1-O1-Bi1	93.61(28)	Nb1-O1-Bi1	93.93(32)

AN		ABNT003		ABNT007		ABNT009	
Nb2-O4-Nb2	158.9(27)	Nb1-O1-Bi1	101.5(7)	Nb1-O1-Bi1	101.4(6)	Nb1-O1-Bi1	101.8(4)
Nb1-O5-Nb1	163.5(14)	Ta1-O1-Ta1	153.6(13)	Ta1-O1-Ta1	153.3(12)	Ta1-O1-Ta1	152.1(7)
Nb1-O6-Nb1	162.6(24)	Ta1-O1-Bi1	93.31(30)	Ta1-O1-Bi1	93.61(28)	Ta1-O1-Bi1	93.93(32)
Nb1-O7-Nb1	156.4(16)	Ta1-O1-Bi1	101.5(7)	Ta1-O1-Bi1	101.4(6)	Ta1-O1-Bi1	101.8(4)
		Bi1-O1-Bi1	104.3(9)	Bi1-O1-Bi1	105.1(8)	Bi1-O1-Bi1	105.0(8)
		Ag2-O2-Nb1	102.5(7)	Ag2-O2-Nb1	102.5(6)	Ag2-O2-Nb1	102.0(4)
		Ag2-O2-Ta1	102.5(7)	Ag2-O2-Ta1	102.5(6)	Ag2-O2-Ta1	102.0(4)
		Ag2-O2-Bi2	0.000(0)	Ag2-O2-Bi2	0.000(0)	Ag2-O2-Bi2	0.000(0)
		Nb1-O2-Nb1	155.0(14)	Nb1-O2-Nb1	155.1(13)	Nb1-O2-Nb1	156.1(8)
		Nb1-O2-Ta1	0.000(0)	Nb1-O2-Ta1	0.000(0)	Nb1-O2-Ta1	0.000(0)
		Nb1-O2-Ta1	155.0(14)	Nb1-O2-Ta1	155.1(13)	Nb1-O2-Ta1	156.1(8)
		Nb1-O2-Bi2	102.5(7)	Nb1-O2-Bi2	102.5(6)	Nb1-O2-Bi2	102.0(4)
		Ta1-O2-Ta1	155.0(14)	Ta1-O2-Ta1	155.1(13)	Ta1-O2-Ta1	156.1(8)
		Ta1-O2-Bi2	102.5(7)	Ta1-O2-Bi2	102.5(6)	Ta1-O2-Bi2	102.0(4)
		Nb1-O3-Nb1	171.7(8)	Nb1-O3-Nb1	171.8(7)	Nb1-O3-Nb1	171.6(8)
		Nb1-O3-Ta1	0.000(0)	Nb1-O3-Ta1	0.000(0)	Nb1-O3-Ta1	0.000(0)
		Nb1-O3-Ta1	171.7(8)	Nb1-O3-Ta1	171.8(7)	Nb1-O3-Ta1	171.6(8)
		Ta1-O3-Ta1	171.7(8)	Ta1-O3-Ta1	171.8(7)	Ta1-O3-Ta1	171.6(8)
		Nb1-O4-Nb1	164.2(8)	Nb1-O4-Nb1	164.2(7)	Nb1-O4-Nb1	163.8(7)
		Nb1-O4-Ta1	0.000(0)	Nb1-O4-Ta1	0.000(0)	Nb1-O4-Ta1	0.000(0)
		Nb1-O4-Ta1	164.2(8)	Nb1-O4-Ta1	164.2(7)	Nb1-O4-Ta1	163.8(7)
		Nb1-O4-Bi1	95.5(6)	Nb1-O4-Bi1	96.3(6)	Nb1-O4-Bi1	96.7(7)
		Nb1-O4-Bi1	96.4(8)	Nb1-O4-Bi1	96.0(7)	Nb1-O4-Bi1	96.2(7)
		Ta1-O4-Ta1	164.2(8)	Ta1-O4-Ta1	164.2(7)	Ta1-O4-Ta1	163.8(7)
		Ta1-O4-Bi1	95.5(6)	Ta1-O4-Bi1	96.3(6)	Ta1-O4-Bi1	96.7(7)
		Ta1-O4-Bi1	96.4(8)	Ta1-O4-Bi1	96.0(7)	Ta1-O4-Bi1	96.2(7

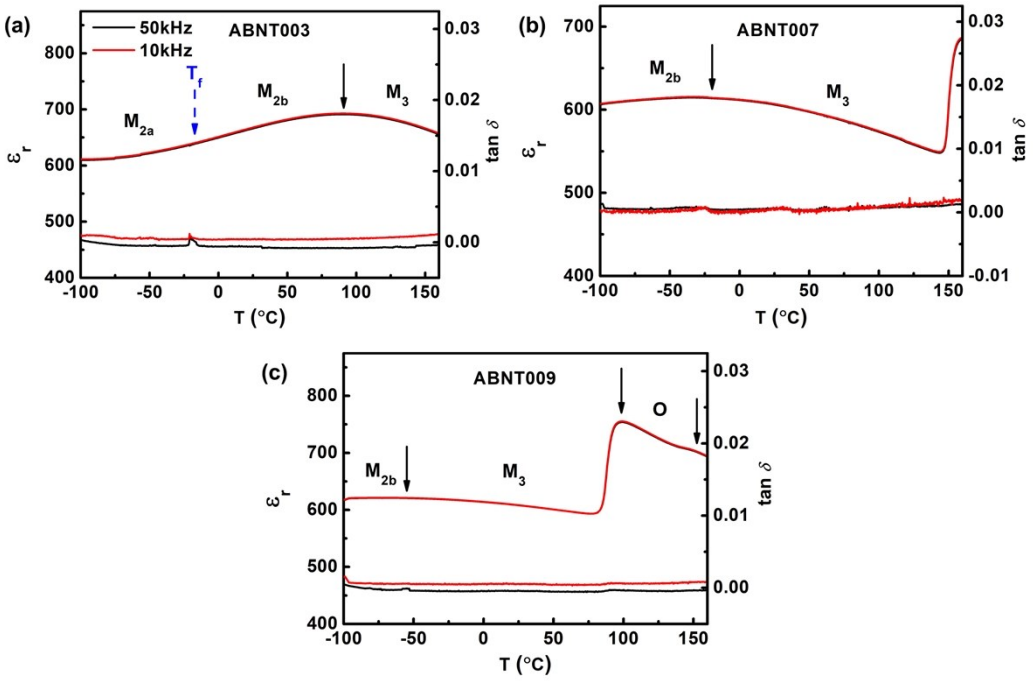

Fig. S2 Low temperature dependence of relative permittivity and dielectric loss in AN and ABNT*x* ceramics.

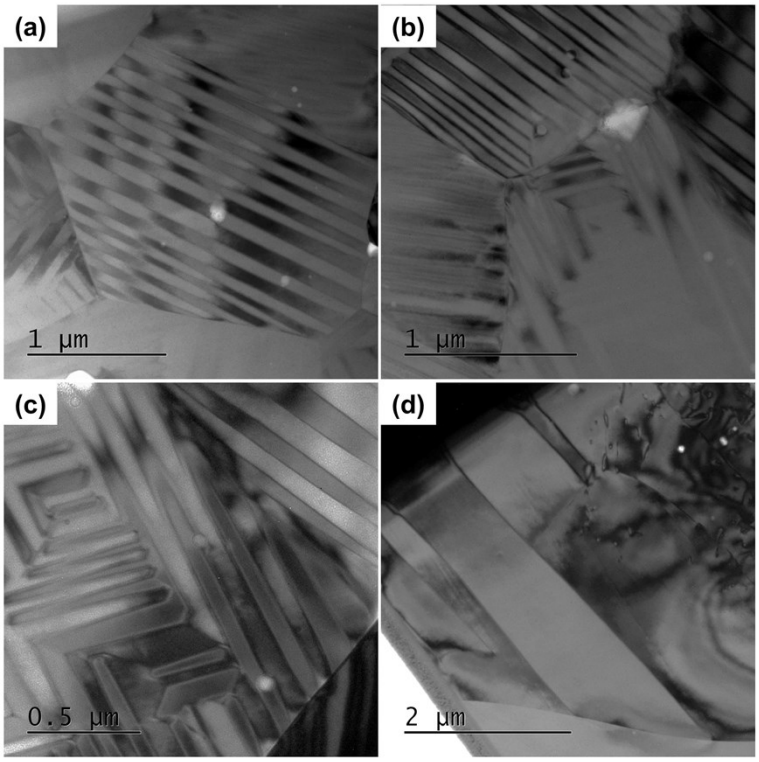

Fig. S3 Bright-field TEM images showing domains of (a-c) ABNT003 and (d) ABNT009 ceramics.

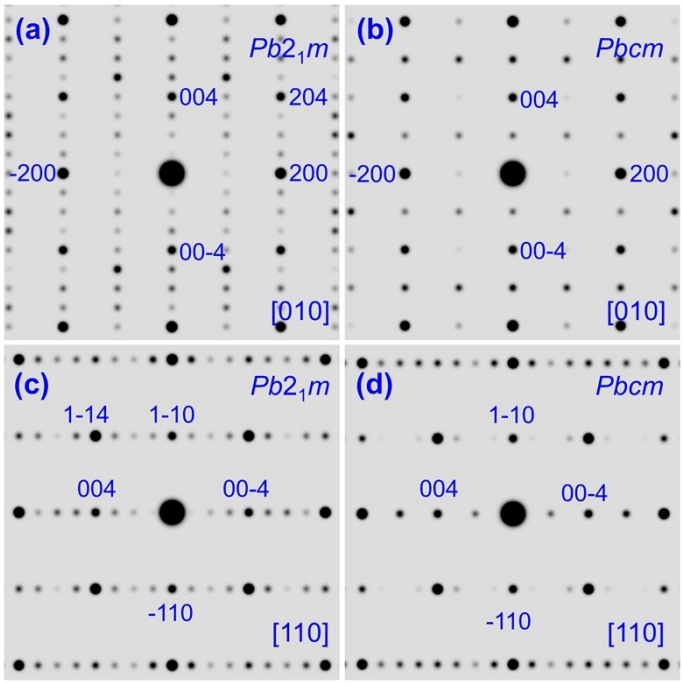

Fig. S4 Calculated TEM diffraction patterns for ABNT003 ceramics using both (a, and c) $Pb2_1m$ and (b, and d) *Pbcm* models along (a, and b) [010] and (c, and d) [110] zone axes.

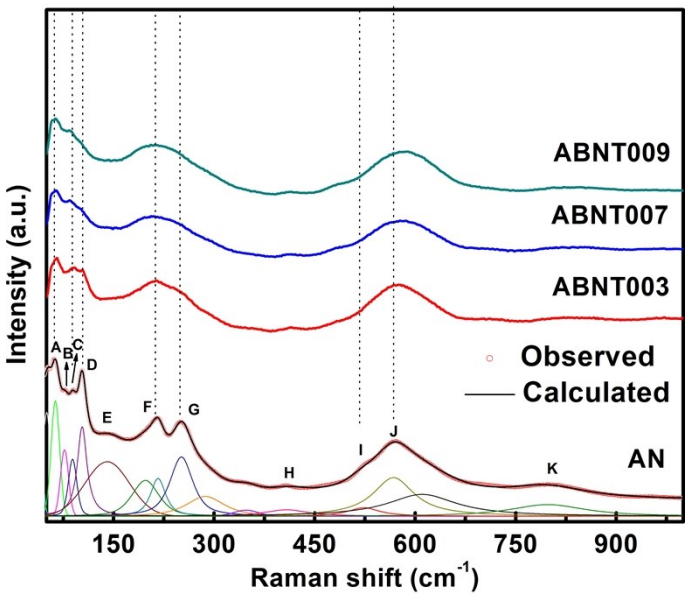

Fig. S5 Raman spectra of AN and ABNT*x* ceramic powders. The fitted peaks are shown in the spectral deconvolution of AN at the bottom.

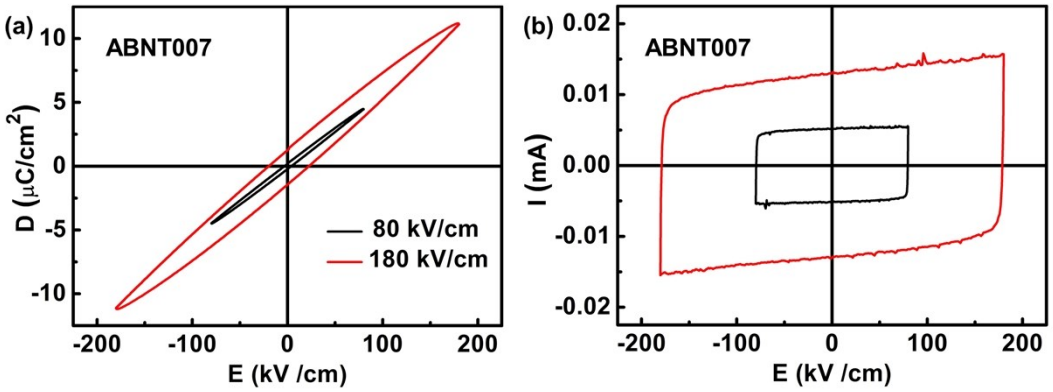

Fig. S6 Ferroelectric D-E and I-E loops measured at 10 Hz for ABNT007 ceramic.

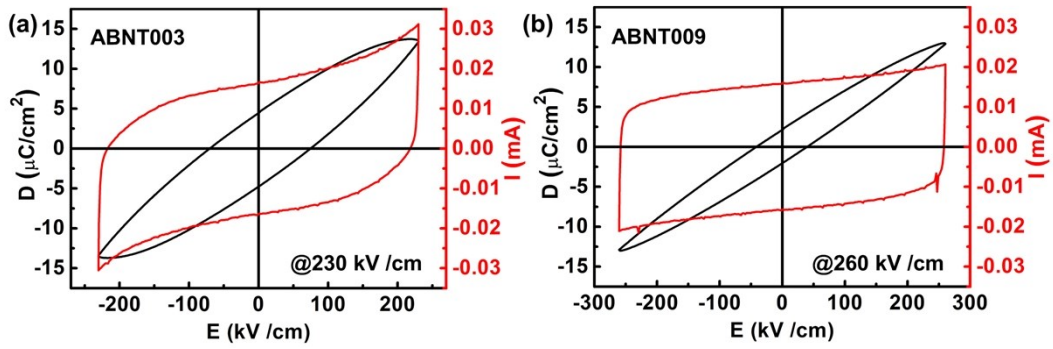

Fig. S7 Ferroelectric D-E and I-E loops measured at 10 Hz for ABNT003 and ABNT009 ceramics.